4.4 Thermal-Hydraulic Design

4.4.1 Design Bases

The objective of the thermal-hydraulic design is to provide adequate heat transfer for the fuel rods and control components that will satisfy standard operational and safety criteria:

- Fuel damage is not expected during normal operation or during anticipated operational occurrences (AOO); however, it is not possible to preclude a very small number of fuel rod failures. The small number of fuel rod failures is within the capability of the plant cleanup system and is consistent with the plant design bases.

- The reactor can be brought to a safe state and kept subcritical with acceptable heat transfer following a postulated accident (PA) with only a small fraction of fuel rods damaged; however, additional fuel damage beyond a small fraction may require considerable outage time before resuming operation.

The following GDC apply to Section 4.4:

- GDC 10 requires that the reactor core and associated coolant, control, and protection systems be designed with appropriate margin so that specified acceptable fuel design limits are not exceeded during any condition of normal operation, including the effects of AOOs. As noted in Section 3.1.2, the reactor core and associated coolant, control, and protection systems have been designed with appropriate margin so that acceptable fuel design limits are not exceeded during steady-state operation or AOOs. This design demonstrates that the reactor will perform its safety functions throughout its design lifetime under all modes of operation.

- GDC 12 requires that the reactor core and associated coolant, control, and protection systems be designed so power oscillations that result in conditions exceeding specified acceptable fuel design limits are not possible or can be reliably and readily detected and suppressed. As noted in Section 3.1.2, power oscillations of the fundamental mode are inherently eliminated by negative Doppler and negative moderator temperature coefficients of reactivity. Oscillations due to xenon spatial effects in the radial, diametral, and azimuthal harmonic overtone modes, are also heavily damped due to the inherent design and the negative Doppler and nonpositive moderator temperature coefficients of reactivity.

4.4.1.1 Departure from Nucleate Boiling Design Basis

By preventing departure from nucleate boiling (DNB), the heat transfer from the fuel cladding to the reactor coolant will prevent cladding damage. Maximum fuel rod surface temperature is not a design basis because it will be within a few degrees of the coolant temperature during operation in the nucleate boiling regime. Limits provided by the reactor control surveillance limitation (RCSL) system and the protection system (PS) demonstrate that the DNB design basis will be met for transients associated with

AOO events. There is additional departure from nucleate boiling ratio (DNBR) margin at rated power operation and during normal operating transients.

Using simplified online DNBR calculations in the RCSL system and PS enables the design criterion to be met. These simplified calculations define a low DNBR for reactor trip (RT) and a limiting condition of operation (LCO) based on DNB. The calculations are based directly on a reconstructed variable that represents the thermal-hydraulic phenomenon to be avoided.

The online calculated values are provided by systems that apply an algorithm to reactor measurements to reconstruct the local conditions, then apply the chosen critical heat flux (CHF) correlations to calculate the CHF. The reconstruction uncertainties and the measurement accuracy are considered when establishing the setpoints for the online calculated DNBR value. The setpoints provide a 95 percent probability, at a 95 percent confidence level, that DNB will not occur during the limiting transient when the stationary online DNBR calculated value is equal to the DNBR thresholds.

4.4.1.2   Fuel Temperature Design Basis

4.4.1.2.1   Design Basis

For normal operation and AOOs there is at least a 95 percent probability, at a 95 percent confidence level, that the fuel melting temperature is not exceeded in any part of the core. The melt temperature relationships for UO_2 and gadolinia fuel are documented in COPERNIC Fuel Rod Design Computer Code (Reference 1). The NRC accepted this code and methodology for use with the U.S. EPR in Codes and Methods Applicability Report for the U.S. EPR (Reference 2).

4.4.1.2.2   Discussion

Fuel rod thermal evaluations are performed at rated power and during transients up to the design limit burnup. The analyses verify that the fuel temperature and integrity design bases presented in Section 4.2.1 are satisfied. The analyses also provide input for the evaluation of Chapter 15 events.

4.4.1.3   Core Flow Design Basis

4.4.1.3.1   Design Basis

A minimum of 94.5 percent of the thermal design flow will pass through the fuel rod region of the core and be effective for fuel rod cooling. Flow through the thimble tubes and leakage from the heavy reflector into the core is considered ineffectual for heat removal.

4.4.1.3.2 Discussion

Core cooling evaluations are based on the thermal design flow entering the reactor pressure vessel (RPV). Under normal operating conditions, a maximum of 5.5 percent of this value is allotted as bypass flow. This includes guide thimble cooling flow, head cooling flow, heavy reflector cooling flow, and leakage to the vessel outlet nozzle.

4.4.1.4 Hydrodynamic Stability Design Basis

The hydrodynamic stability design basis is that modes of operation associated with normal operation and AOO events do not lead to hydrodynamic instability.

4.4.1.5 Additional Considerations

The design bases in Section 4.4.1.1 and Section 4.4.1.2, along with the fuel cladding and fuel assembly design bases presented in Section 4.2.1, are comprehensive so that no additional limits are required.

Design bases on fuel pellet properties, pellet-cladding gap characteristics, coolant flow velocity and distribution, and moderator void fraction are not individually specified. Each parameter is incorporated into the thermal-hydraulic analyses used to show concurrence with the design bases (Sections 4.4.1.1, 4.4.1.2, and 4.2.1).

During AOO events and normal operation, heat transfer by nucleate boiling in the hot fuel assembly maintains the cladding surface temperature within a few degrees of the coolant temperature. Consequently, a design basis on cladding surface temperature is not required for AOO events and normal operation. A cladding temperature limit is applied to specific PA events, as described in Section 15.6.5, to avoid excessive cladding oxidation.

4.4.2 Description of Thermal-Hydraulic Design of the Reactor Core

4.4.2.1 Summary Comparison

Values of pertinent parameters along with DNB ratios, reactor coolant system (RCS) temperatures, and linear heat generation rates are presented in Table 4.4–1—Thermal and Hydraulic Design Data.

4.4.2.2 Critical Heat Flux Ratios

The minimum DNBR for nominal, rated power conditions is given in Table 4.4-1. The DNBRs are calculated with the CHF correlations and definitions described in Sections 4.4.4.1.1 and 4.4.4.1.2. The LYNXT Core Transient Thermal-Hydraulic Program (Reference 3) is described in Section 4.4.4.5.1 and is used to determine the flow distribution in the core and the local conditions in the hot channel for use in the CHF

correlations. The NRC accepted this code and methodology for use with the U.S. EPR in the Codes and Methods Applicability Topical Report (Reference 2).

4.4.2.3   Linear Heat Generation Rate

The core average and maximum heat flux and linear power are given in Table 4.4-1. The methodology used to calculate the maximum linear heat generation rate is provided in Section 4.3.2.2.

4.4.2.4   Void Fraction Distribution

The calculated core average and hot subchannel maximum and average void fractions are presented in Table 4.4–2—Core Void Fractions. Curves showing the predicted axial variations of quality and void fraction for the limiting subchannel are provided in Figure 4.4–1—Axial Distribution of Quality and Void Fraction in the Limiting Subchannel. Figure 4.4–2—Radial Distribution of Quality and Void Fraction at the Core Exit shows the core-wide radial distribution of maximum values of quality and void fraction. The void fraction models used in the analysis are also described in Reference 3.

4.4.2.5   Core Coolant Flow Distribution

Assembly average coolant mass velocity and enthalpy at various core elevations are shown in Figures 4.4-3—Assembly Average Flow and Enthalpy Distribution at Core Inlet (1/8 Core), Figure 4.4–4—Assembly Average Flow and Enthalpy Distribution at Core Mid-plane (1/8 Core), and Figure 4.4-5—Assembly Average Flow and Enthalpy Distribution at Core Exit (1/8 Core). These distributions are for nominal, full power conditions with a typical radial power distribution. The LYNXT analysis utilizes a uniform core inlet temperature and the four pump inlet flow distribution described in Section 4.4.2.6.2.

4.4.2.6   Core Pressure Drops and Hydraulic Loads

4.4.2.6.1   Bypass Flow

Bypass flow is described in Section 4.4.4.2.1.

4.4.2.6.2   Core Inlet Flow Mal-Distribution

The core inlet flow distribution has been determined using a one-seventh scale-model testing of the RPV lower internals. Nominal distributions for operation with four pumps and three pumps were determined from these tests. Two flow zones are modeled according to the placement of the flow distribution device (FDD) below the lower core plate (refer to Section 3.9.5). The location of the FDD in relationship to the core is shown in Figure 4.4–6—Location of Flow Distribution Device Beneath the

Core. The core inlet flow distribution is characterized as non-uniform across the core inlet with higher flows in the central region of the core.

As coolant flows through the fuel assembly, the distribution rapidly adjusts due to the open lattice structure of the fuel assemblies. This re-distribution occurs within the first few grid spans and thus has minimal effect on the DNBR in the hot channel. In the LYNXT analyses, a flow mal-distribution penalty is conservatively applied to the hot fuel assembly.

4.4.2.6.3   Core and Vessel Pressure Drops

The pressure drop across the entire RPV during hot conditions and at the best estimate RCS flow rate represents the unrecovered losses from the cold leg nozzles, the downcomer and lower plenum, the cower core support plate, the core, and the upper plenum. The analytical model used to calculate pressure drops is described in Section 4.4.2.7.2.

4.4.2.6.4   Hydraulic Loads

Bounding hydraulic loads on vessel components and fuel assemblies are evaluated with the mechanical design flow rate. The analysis of the fuel assemblies also utilizes the minimum core bypass flow.

Hydraulic loads on the fuel assemblies are evaluated for nominal operating conditions and for cold shutdown conditions (start of the fourth reactor coolant pump (RCP)). Fuel assembly hydraulic loads in transient conditions are bounded by a postulated 20 percent increase in reactor coolant system flow rate.

4.4.2.7   Correlations and Physical Data

4.4.2.7.1   Surface Heat Transfer Coefficients

Single-phase forced convection heat transfer coefficients are obtained from a modified Dittus-Boelter correlation (Reference 4 and Reference 5), with the properties evaluated at bulk fluid conditions:

$$h = 0.023 \frac{k}{D_H} \left(R_e\right)^{0.8} \left(\mathrm{Pr}\right)^{0.4}$$

Where:

h=heat transfer coefficient (Btu/hr-ft^2-°F)

D_H =hydraulic diameter (ft)

k=thermal conductivity (Btu/hr-ft-°F)

Re=Reynolds number

Pr=Prandtl number

This correlation has been shown to be conservative for rod bundles with pitch-to-diameter ratios in the range of the U.S. EPR (Reference 5).

The onset of nucleate boiling is predicted by the Jens and Lottes correlation (Reference 6). After this occurrence, the forced convection heat transfer coefficient is determined by:

$$h = \frac{q''}{\left[\frac{60\left(\frac{q''}{10^6} \right)}{e^{\left(\frac{P}{900} \right)}} \right] + T_{sat} - T_{Bulk}}$$

Where:

h=heat transfer coefficient

q"=wall heat flux (Btu/hr-ft^2)

P=pressure (psia)

T_{bulk}=bulk fluid temperature (°F)

T_{sat}=saturation temperature of coolant at P (°F)

4.4.2.7.2   Total Core and Vessel Pressure Drop

Unrecoverable pressure drops are present from geometry changes in the fluid flow path and friction resulting from viscous drag. For the pressure drop analysis, the fluid is assumed to be incompressible, turbulent, single-phase water. These assumptions apply to both the core and vessel pressure drop calculations to establish the RCS loop flow rate. The core pressure drop is determined by the Darcy equation:

$$\Delta P_L = (K + f \frac{L}{D_e}) \frac{\rho V^2}{2g_c(144)}$$

Where:

ΔP_L=pressure drop (lbf/in.^{2})

K=form loss coefficient (dimensionless)

f=friction loss coefficient (dimensionless)

L=length (ft)

D_e=equivalent diameter (ft)

ρ=fluid density (lbm/ft^3)

V=fluid velocity (ft/s)

g_c=32.174 (lbm-ft/lbf-s^2)

Fluid density is assumed to be constant at the appropriate value for each component in the core and vessel. Because of the complex core and vessel flow geometry, precise analytical values for the form and friction loss coefficients are not available.

The total unrecoverable vessel pressure drop is 30.10 psid during hot conditions at the best estimate RCS flow rate.

Testing of the RCS loop flow rates are made prior to criticality, as described in Section 4.4.5.1, to verify that flow rates used in the design of the RCS are conservative. Refer to Section 14.2 for a description of preoperational testing.

4.4.2.7.3 Void Fraction Correlation

The void fraction correlations used in the LYNXT analyses are documented in the LYNXT Topical Report (Reference 3).

4.4.2.8 Thermal Effects of Operational Transients

Section 4.4.6.4 gives a description of the low DNBR LCO and the low DNBR trip function. These functions provide the required DNB protection for both normal operation and AOO events that are slow with respect to fluid transport delays in the RCS. Additional protective functions are provided for fast events and events initiated from hot zero power. The functions are described in Section 7.2 and their use in the safety analysis is described in Chapter 15.

Section 4.4.6.5 gives a description of the linear power density (LPD) LCO and the high linear power density (HLPD) trip function. These functions provide protection against centerline fuel melting and cladding strain for both normal operation and AOO events that can be detected by the incore instrumentation. Additional protective functions are provided for extremely fast events, for example control rod ejection. The functions are described in Section 7.2 and their use in the safety analysis is described in Chapter 15.

4.4.2.9 Uncertainties in Estimates

4.4.2.9.1 Uncertainties in Fuel and Cladding Temperatures

Fuel and cladding temperatures are calculated with the COPERNIC code. The fuel temperature predictions have been extensively benchmarked to experimental and postirradiation examination data for a variety of fuel rod designs and operating conditions (Reference 1). The bounding fuel temperature predictions, at 95 percent probability and 95 percent confidence level, account for fuel fabrication uncertainties and uncertainties in the physical models and the design code. The effect of fuel densification is included in the calculation of the total uncertainty. Additional uncertainties due to manufacturing tolerances and the determination of the local power density are captured within the heat flux hot channel factor (HCF) (F_Q).

Uncertainty in the cladding temperature calculation is primarily determined by uncertainty in the oxide layer thickness. Operation within the nucleate boiling regime means that the cladding surface temperature is within a few degrees of the coolant temperature. Consequently, uncertainties in the cladding temperatures are not significant.

4.4.2.9.2 Uncertainties in Pressure Drops

The total core pressure drop based on the best-estimate flow, as described in Section 5.1, is provided in Section 4.4.2.7.2. Minimum and maximum values were calculated for the core bypass flow. The minimum and maximum core bypass values consider the uncertainties allowed by manufacturing tolerances.

The primary purpose of calculating the RPV pressure drops is to determine the RCS loop flowrates. To verify the analyzed RCS flow rate, testing will be performed prior to criticality, as described in Section 4.4.5.1.

4.4.2.9.3 Uncertainties Due to Inlet Flow Mal-Distribution

Uncertainties in the inlet flow distribution are addressed through the application of a bounding inlet flow mal-distribution penalty to the hot assembly.

4.4.2.9.4 Uncertainty in CHF Correlation

The uncertainty in the CHF correlation represents the probability of not being in DNB based on the statistics of the CHF test data. The CHF correlation design limit accounts for this uncertainty in The ACH-2 CHF Correlation for the U.S. EPR (Reference 7) and Application of The BWU Critical Heat Flux Correlations (Reference 8).

4.4.2.9.5 Uncertainties in DNBR Calculations

A statistical approach is used to combine the uncertainties affecting the DNBR. The uncertainties presenting a random feature and a probability law precisely known are statistically treated, the others are treated deterministically. Additional details are provided in Incore Trip Setpoint and Transient Methodology for U.S. EPR (Reference 9).

4.4.2.9.6 Uncertainties in Flow

Core thermal performance analyses utilize the thermal design flow with a maximum value of core bypass. This accounts for both prediction and measurement uncertainties and conservatively bounds the nominal operation of the plant.

4.4.2.9.7 Uncertainties in Hydraulic Loads

The analysis of the hydraulic loads utilizes the mechanical design flow rate with a minimum value of core bypass. This accounts for both prediction and measurement uncertainties and conservatively bounds the nominal operation of the plant. Enveloping hydraulic loads on the fuel assembly are evaluated in normal operation for cold shutdown conditions (start of the fourth RCP) and in transient conditions for a 20 percent pump overspeed transient. Uncertainties are handled statistically using the methodology from Statistical Fuel Assembly Hold Down Methodology (Reference 10). The NRC accepted this code and methodology for use with the U.S. EPR in the Codes and Methods Applicability Topical Report (Reference 2).

4.4.2.9.8 Mixing Coefficient Uncertainty

Uncertainties in the mixing coefficient are addressed through the application of bounding coefficients in the LYNXT analyses.

4.4.2.10 Flux Tilt Considerations

During normal operation, the radial power distribution in the core remains relatively flat with zero azimuthal imbalance (i.e., flux tilt). Significant azimuthal imbalances caused by an asymmetric perturbation, such as control rod drop, are analyzed separately in Chapter 15. This description is confined to azimuthal imbalances caused by x-y xenon transients and normal maneuvering.

The design value of the enthalpy rise HCF $F_{\Delta H}$ is sufficiently conservative to account for azimuthal imbalances within the LCO bounds (refer to Section 16.3.2). The design value of F_Q does not include a specific allowance for azimuthal imbalances.

When the indicated azimuthal imbalance exceeds the limit, corrective action is required. The procedure to be followed is provided in Technical Specification 3.2.5 in

Chapter 16. The azimuthal imbalance limit maintains the validity of the core design and confirms the design values used in the safety analysis.

4.4.3 Description of the Thermal and Hydraulic Design of the Reactor Coolant System

4.4.3.1 Plant Configuration Data

Plant configuration data for the thermal-hydraulic and fluid systems external to the core are provided in Chapters 5:

- The RCS is described in Section 5.1. RCS layout drawings, P&IDs, and elevations drawings are included as figures in Section 5.1. The RCS configuration is shown in Figure 5.1–2—RCS Layout.

- Listing of RCS valves is provided in Table 3.2-1—Classification Summary and the RCS piping layout is shown in Section 5.1.

- Flow for each loop is provided in Table 5.1–1—RCS Design and Operating Parameters. Flow used in the evaluation of the core is addressed throughout this section.

- RCS volume, including the pressurizer, is presented in Table 5.1-1.

- RCS components are described in Section 5.4.

- An RCS elevation drawing is provided in Figure 5.1-3—RCS Elevation.

- A description of the SIS, including figures with basic piping dimensions, is included in Section 6.3.

4.4.3.2 Operating Restrictions on Pumps

The minimum net positive suction head (NPSH) is established before operating the reactor coolant pumps. RCS pressure and temperature are verified to meet the requirements for minimum NPSH of the RCPs listed in Table 5.4-1—Reactor Coolant Pump Design Data.

4.4.3.3 Power-Flow Operating Map (BWR)

Not applicable to the U.S. EPR.

4.4.3.4 Temperature-Power Operating Map (PWR)

The relationship between the RCS average temperature and core power between zero and 100 percent power is shown in Figure 4.4-7—Average RCS Temperature vs. Core Power. The effects of reduced core flow from inoperative pumps are described in Sections 15.2.6 and 15.3. Power production is not permitted for the U.S. EPR with one or more pumps out of service.

4.4.3.5 Load-Following Characteristics

Load follow using control rods and boron dilutions or additions are described in Section 4.3.2.4.15.

4.4.3.6 Thermal and Hydraulic Characteristics Summary Table

A summary of the thermal and hydraulic characteristics of the reactor is presented in Table 4.4-1.

4.4.4 Evaluation

4.4.4.1 Critical Heat Flux

4.4.4.1.1 CHF Correlations

Two CHF correlations are applied to the high thermal performance (HTP) fuel assemblies for the U.S. EPR. The ACH-2 correlation (Reference 7) is applied downstream of HTP mixing grids and the BWU-N correlation (Reference 8) is applied downstream of the high mechanical performance (HMP) structural grids.

The ranges and limitations of the ACH-2 CHF correlation and the BWU-N CHF correlation are presented in Reference 7 and Reference 8, respectively.

4.4.4.1.2 Definition of DNBR

The DNBR for both a typical and thimble cell is defined as:

$$DNBR = \frac{q''_{CHF}}{q''_{local}}$$

Where:

$$q''_{CHF} = \frac{q''_{correlation}}{F}$$

q''_{CHF} =predicted critical heat flux

$q''_{correlation}$=critical heat flux from CHF correlation (ACH-2 or BWU-N)

F=nonuniform axial heat flux factor

q''_{local}=actual heat flux

4.4.4.1.3   Mixing Technology

In a rod bundle, the flow channels formed by four adjacent fuel rods are open to each other through the gap between two neighboring fuel rods. There is cross-flow between channels because of the pressure differential between the channels. The mixing effect reduces enthalpy rise in the hot channel.

In the energy balance equation of the LYNXT code, a term is included to model the turbulent enthalpy exchange between adjacent channels. This term is proportional to the enthalpy difference between adjacent channels. In the proportionality factor, a coefficient appears called the "turbulent mixing coefficient."

The value of this coefficient is determined by performing a series of thermal mixing tests for a particular spacer grid design. The coefficients used in the LYNXT thermal-hydraulic analyses conservatively bound the performance of the respective spacer grid designs and are consistent with the development of the CHF correlations: ACH-2 for HTP spacer grids and BWU-N for HMP spacer grids.

4.4.4.1.4   Hot Channel Factors

Two hot channel factors (HCFs) are defined for use with the U.S. EPR (see Section 4.3). The heat flux HCF (F_Q) is defined as the ratio of the core maximum heat flux to the core average heat flux. It defines the maximum localized heat flux in the core. The enthalpy rise HCF ($F_{\Delta H}$) is defined as the ratio of the maximum to core average integrated heat flux along a channel. This factor defines the maximum fuel rod power in the core.

The following items define the engineering HCF:

- The heat flux engineering HCF (F_Q^E) accounts for variations in enrichment, pellet density and diameter, surface area of the cladding, and eccentricity of the gap between the pellet and the cladding. This factor is statistically determined by an evaluation of the coefficient of variation using the nominal values for the relative parameters and their tolerances. It is used for evaluations of the maximum heat flux. This factor is not applied to DNBR analyses since the localized, short lived variation of heat flux has minimal affect.

- The enthalpy rise engineering HCF ($F_{\Delta H}^E$) accounts for variations in pellet diameter, density, enrichment, fuel rod diameter, fuel rod pitch, and fuel rod bowing. The effects of inlet flow mal-distribution, flow redistribution, and flow mixing are accounted for separately in the LYNXT modeling. The HCF is statistically determined by an evaluation of the coefficient of variation using the nominal values for the relative parameters and their tolerances. It is used in the LYNXT analyses for DNBR.

4.4.4.1.5 Effects of Rod Bow and Assembly Bow

Fuel rod bow and fuel assembly bow are described in Fuel Rod Bowing in Babcock & Wilcox Fuel Designs (Reference 11) and in Extended Burnup Evaluation (Reference 12). This methodology was extended to the U.S. EPR in the Codes and Methods Applicability Topical Report (Reference 2). The effects of bowing, both fuel rod and assembly, are manifested as a statistically combined penalty on the HCFs. Separate penalties are determined for heat flux (F_Q) and enthalpy rise ($F_{\Delta H}$). These penalties are applied to analyses of the maximum heat flux and DNBR.

4.4.4.2 Core Hydraulics

4.4.4.2.1 Flow Paths Considered in Core Pressure Drop and Thermal Design

The core bypass flow has been determined by calculation based on drawings of the RPV, RPV internals, and the fuel assemblies. The following flow paths for core bypass are considered:

- Flow through the gap between the RPV and upper internals into the upper head for head cooling purposes.

- Flow entering the hot leg as a result of the gap between the core barrel and the RPV.

- Flow passing between the periphery of the core and the inside of the heavy reflector.

- Flow through the heavy reflector and between the heavy reflector and the core barrel.

- Flow through fuel assembly thimbles.

The above core bypass flows have been evaluated to confirm the design value of the core bypass flow is met. Based on the calculation, the maximum assumed core bypass flow is 5.5 percent.

4.4.4.2.2 Inlet Flow Distributions

The flow exiting the RPV inlet nozzles will have a mal-distribution factor in the downcomer from the asymmetry of the RPV inlet nozzles. The mal-distribution of the flow is considered insignificant and has been neglected from the thermal-hydraulic analysis of the RPV.

The core inlet flow distribution has been determined through flow testing with a one-seventh scale-model of the RPV lower internals. The results of the flow tests for both full and partial pump operation are addressed in Section 4.4.2.6.2.

4.4.4.2.3 Emperical Friction Factor Correlations

The isothermal friction factor used in the LYNXT thermal-hydraulic code (Reference 3) for flow in the axial direction parallel to the fuel rods is based on the Moody friction factor curves. The relationship is a function of the absolute surface roughness, the equivalent hydraulic diameter, and the Reynolds number. Corrections are applied to the isothermal friction factor for the effects of heat addition and two-phase flow. The increase in friction loss is modeled with a multiplier applied to the single-phase friction factor. The corrections to the isothermal friction factor include empirical correlations for diabatic single-phase liquid flow, subcooled boiling, and bulk boiling flow.

The lateral flow between subchannels and assemblies is modeled with a crossflow resistance term. The lateral resistance is a function of the rod geometry and centroidal spacing.

4.4.4.3 Influence of Power Distributions

Core power distribution is a function of many variables: fuel design, loading pattern, control rod worth and position, and fuel depletion. The core power distribution is divided into two components that describe the radial and axial variations. Core radial enthalpy rise distribution ($F_{\Delta H}$) is representative of the integral of power in each channel and is important for DNB analyses because of the effect on local coolant conditions (pressure, mass flow, and quality). The magnitude of DNBR depends on the enthalpy rise to a given elevation, while the elevation of minimum DNBR depends on the axial power shape. DNBR analyses are performed by setting the hot fuel rod to the maximum predicted $F_{\Delta H}$ value of 1.70 presented in Table 4.3-1 and applying a conservative radial power distribution in the remainder of the hot assembly and the core. Axial power distributions are selected to conservatively bound operation within the axial power shape LCO. A single axial power shape is applied to the entire core.

Core thermal margin predictions are performed with the LYNXT code (see Section 4.4.4.5.1). Sensitivity analyses are performed varying the number of channels used to model the core, varying the peaking gradients both within the limiting assembly and in the remainder of the core, and varying the location of the limiting fuel rod. These sensitivity studies identify the core model used with the limiting fuel rod to calculate the thermal margin of the reactor. The combined use of the limiting axial and radial power distributions and conservative core model are used to evaluate the thermal margin of the reactor.

The core-related instrumentation and control (I&C) protection functions protect the core against penalizing power distributions. The power density distribution of the hot channel is directly derived from the nuclear incore instrumentation by self-powered

neutron detectors (SPND), which are described in Sections 4.4.6.1 and 4.4.6.4. Additional SPND details are provided in Reference 9.

4.4.4.4 Core Thermal Response

The thermal-hydraulic characteristics of the core under steady-state operating conditions are presented in Table 4.4-1. Core thermal response during AOOs and PAs is presented in Chapter 15.

4.4.4.5 Analytical Methods

The objective of the reactor core thermal design is to demonstrate acceptable performance in relation to the design bases established in Section 4.4.1, and to show that the core safety limits given in the Technical Specifications of Chapter 16 are not exceeded. It considers variations and uncertainties in the nuclear design, combined with engineering factors, to account for flow effects and manufacturing tolerances.

4.4.4.5.1 Reactor Coolant System Flow Determination

The reactor coolant system flow rate is determined using standard steady-state hydraulics calculations. A flow network model of the reactor vessel, reactor coolant system piping, and steam generator is developed. All four loops are modeled. Reactor coolant pump head-capacity curves are provided by the pump vendor. These are based on previous design experience that has been confirmed with test data. Reactor vessel hydraulic resistances, excluding the core, are determined from scale-model testing. Core form and friction losses are based on fuel assembly tests. Reactor coolant piping hydraulic losses are relatively minor and are consistent with operating plant values. The steam generator losses are dominated by tube friction and are based on operating plant experience.

The best estimate, thermal-hydraulic and mechanical reactor coolant system flow rates are provided in Table 5.1-1. The best estimate flow is 4.1 percent greater than the thermal-hydraulic flow and approximately 8.0 percent less than the mechanical flow. The measured RCS flow uncertainty is less than 2.5 percent and is based on a secondary heat balance uncertainty of less than 0.5 percent. It also includes hot leg and cold leg temperature instrument uncertainties, as well as the effects of hot leg streaming on the temperature uncertainty.

4.4.4.5.2 Core Analysis

Design analyses are performed using the LYNXT computer code (Reference 3). LYNXT is a versatile core thermal-hydraulic transient program based on the COBRAIV-1 code. Typical applications include core-wide flow and enthalpy predictions, subchannel DNBR calculations, transient DNBR and fuel temperature calculations, and pressure drop/cross-flow velocity calculations. LYNXT also contains

an implicit pressure-velocity (PV) algorithm capable of handling low, reverse, and recirculating flows. In addition to DNBR and fuel temperature analyses, LYNXT can be used to:

- Analyze baffle gap jetting, including experimental benchmarks.

- Perform steaming rate calculations.

- Calculate pressure drops.

- Calculate cross-flow velocities and general flow distributions.

- Assess thermal mixing.

- Reduce CHF data.

- Evaluate guide tube boiling.

LYNXT performs one-pass analyses where the hot subchannel, adjacent subchannels, partial bundles, and groups of bundles are all modeled in a single simulation. DNBR analyses are performed by setting the hot fuel rod to the Technical Specification limit for $F_{\Delta H}$ and applying a conservative radial power distribution in the remainder of the hot assembly and the core. Sensitivity studies have demonstrated that the LYNXT DNBR results are not significantly affected by the radial power distribution in the core for the same $F_{\Delta H.}$

Axial power distributions are selected to conservatively bound operation within the axial power shape LCO. A single axial power shape is applied to the entire core.

The LYNXT analyses also account for the following uncertainties and penalties to provide a conservative calculation of minimum departure from nucleate boiling ratio (MDNBR):

- Measurement uncertainties and control bands on system conditions (e.g., power, pressure, and temperature).

- Penalties for fuel rod and fuel assembly bow.

- Core inlet flow mal-distribution penalty applied to the hot fuel assembly.

- Conservative value for the thermal mixing coefficient.

- Engineering HCFs applied to the hot rod and subchannel.

4.4.4.5.3   Steady State Analysis

The online DNB monitoring and surveillance system keeps the MDNBR during normal operation above the DNB LCO setpoint. The DNB LCO is set to provide

---

sufficient initial DNB margin for AOO and PA events that are not mitigated by the low DNBR protection functions. This must be balanced by allowing enough operational flexibility between the DNB LCO setpoint and the MDNBR at normal operating conditions. The methodology used to determine the DNB LCO setpoint is described in Reference 9.

Table 4.4-1 lists the DNB LCO setpoint and the MDNBR at normal operating conditions. Ample margin exists between the setpoint and the nominal condition.

4.4.4.5.4 Transient Analysis

The U.S. EPR transients analyzed and the associated acceptance criteria are presented in Chapter 15. The transient methodology for the low DNBR RT, the DNB LCO, the high linear power density (HLPD) RT, and the LPD LCO are described in Reference 9.

4.4.4.5.5 Thermo-Hydrodynamic Stability

Flow in heated boiling channels is susceptible to several forms of thermo-hydrodynamic instability. These instabilities are undesirable because they may cause thermal-hydraulic conditions that reduce the margin to CHF during steady-state flow conditions or induce the vibration of core components. Therefore, a design criterion stating that conditions during normal operation and AOOs shall not lead to thermo-hydrodynamic instabilities has been established.

The U.S. EPR design was evaluated for its susceptibility to a wide range of potential thermo-hydrodynamic instabilities. This design has ample margin to the conditions that could lead to thermo-hydrodynamic instabilities. The features that enhance stable fluid flow conditions include:

- Rod bundle core configuration: resists parallel channel instability.

- Highly subcooled operation: a power/flow margin to saturation of nearly 50 percent avoids bulk boiling, thus preventing two-phase driven dynamic instabilities.

- High pressure operation: reduces density-driven effects associated with localized steam formation.

- Core channel pressure drop flow curve has a positive slope while the reactor coolant system pump head flow curve is negative: prevents Ledinegg flow excursion instability.

- Margin to CHF: avoids boiling crisis and film-boiling-induced instabilities.

- Low boiling number: provides a factor of eight margin to the inception threshold for acoustic or density waves.

- UO_2 fuel with a long time constant: resists void-reactivity feedback coupling with thermo-hydrodynamic oscillations.

Based on these conclusions, the U.S. EPR will not experience thermo-hydrodynamic instabilities during normal operation and AOOs.

4.4.4.5.6   Fuel Rod Behavior Effects from Coolant Flow Blockage

As coolant flows through the RPV, there are a number of obstructions in the flow path which cannot be passed by loose parts present in the system.

The following core structures protect the core against loose parts of various sizes: the lower core internals, the lower core plate, the fuel assembly lower end fitting (including a debris filter), and the lower spacer grids upstream of the active length. As a result of these structures, only insignificantly small parts are capable of reaching the location where the minimum DNBR occurs in the core.

A blockage of individual openings of the internals results in the deflection of flow. The equalizing effect of the downstream internals compensates for the resulting flow distribution.

There is no adverse effect of a single flow blockage on the thermal-hydraulic behavior of the reactor core.

4.4.5   Testing and Verification

4.4.5.1   Tests Prior to Initial Criticality

An RCS flow test is performed following fuel loading but before initial criticality. RCS loop pressure data are collected during this test. Testing is described in Section 14.2. This includes the recommendations of RG 1.68, as it relates to measurements and the confirmation of thermal-hydraulic design aspects.

4.4.5.2   Initial Power and Plant Operation

Core power distribution measurements will be taken at various power levels during initial power and plant operation, as described in Section 14.2. These tests are used to confirm that conservative peaking factors were used in performing the thermal-hydraulic analyses of the core.

4.4.5.3   Component and Fuel Inspections

Component and fuel inspections are performed following fabrication, as addressed in Section 4.2.4.3. Parameters critical to thermal-hydraulic analyses are measured to verify that the engineering HCFs used in the design analyses are conservative.

4.4.6 Instrumentation Requirements

4.4.6.1 Fixed Incore Instrumentation

The U.S. EPR utilizes a fixed incore power distribution detector (PDD) system comprised of 72 SPNDs distributed at 12 radial core locations with six detectors distributed axially in each radial location, as shown in Figure 4.4–8—Arrangement of Incore Instrumentation (Top View). The primary function of the SPNDs is to accurately and continuously assess the three-dimensional power density distribution and peak power density in the U.S. EPR core. The incore instrumentation also provide the protection and safety monitoring system the signals necessary for monitoring core exit temperatures. The thermocouples are located in the same thimble locations as the SPNDs.

The PDD system is responsible for providing continuous power peaking signals to the PS and reactor control, surveillance, and limitation system (RCSL). That is, the signals of the SPNDs are used for core surveillance (LCO and Limitation) as well as for core protection (trip setpoints). Each detector string, consisting of the six axial detectors, is assigned a surveillance zone defined by axial boundaries in the core. The axial zone boundaries are chosen so that they sufficiently monitor the entire axial length of the core. A detailed description of the surveillance zone determination process for DNBR monitoring is provided in Reference 9.

The SPNDs have a fast response time. The number and the distribution of the SPNDs within the core allow the system to detect and assess local power density increases caused by flux and power redistributions that occur under non-steady-state conditions. The incore detector system design also makes allowance for a proper (functional) signal redundancy. As core burnup progresses, the power-to-signal ratio and the reference power distribution changes. Therefore, calibration of the SPNDs to reference conditions is performed at regular intervals.

POWERTRAX/E (Reference 13), the U.S. EPR online core monitoring software, is designed to produce the SPND calibration factors based on reference aeroball measurements. Reference values for this calibration are local power and hot channel power densities within a section of the core volume assigned to each SPND provided by the aeroball system. Under any conditions, SPNDs change with the neutron flux at the detector location. As a consequence, the calibrated SPND signals are able to follow or track the linear heat generation rate distribution in the core. These signals are used for core control, limitation, and protection purposes. They are processed together with other selected process variables to yield continuous monitoring signals representative of core conditions.

For neutron flux measurement, incore neutron detectors are more accurate than excore neutron detectors, especially with the large size and the heavy reflector of the U.S. EPR core. The PDD system is designed to:

- Directly measure changes in power density.

- Provide increased accuracy of localized power measurements under normal and transient operating conditions.

- Provide increased core surveillance, limitation, and protection information.

- Provide superior measurement of core conditions for peak power density, DNBR, and axial offset.

4.4.6.2   Aeroball Measurement System

The aeroball measurement system (AMS) is an electromechanical, computer-controlled, online flux mapping measurement system based on movable activation probes (aeroballs). The AMS allows for fast, on-demand power distribution measurement. It determines the relative neutron flux density distribution over the entire active core height at 40 fixed positions. A dedicated system computer controls the entire measuring and testing process and measures the count rates from the measured pulses. The AMS calculates the adjusted count rates from the measurement by applying correction factors for specific known events that occur during the flux mapping process, such as decay of the activity during the measuring procedure, residual activities, and scattering effects. Figure 4.4–9—Overview of the Aeroball Measurement System provides a schematic of the AMS. The main features of the AMS are:

- Near instantaneous survey of core status, with activation times of approximately three minutes, allows for measurements during load ramps.

- Time interval between two measurements can be as short as 10 minutes.

The AMS provides data that allow the online core monitoring software, POWERTRAX/E, to calibrate SPNDs and obtain three-dimensional power density distributions that allow for:

- Core conformity verification during startup after refueling.

- SPND calibration at reference core conditions.

- Verification of core design predictions.

- Verification of core behavior over cycle burnup.

- Determination of three-dimensional flux and power density distribution.

- Determination of key safety parameters, (e.g., peak power density, and steady state DNBR margins).

- Checking for the tracking accuracy of the PDD system under semi-transient conditions.

The aeroball probes are carried and distributed over the core by 12 incore lances. Each incore lance bears up to four aeroball fingers and one SPND finger as shown in Figure 4.4-10—Arrangement of Incore Instrumentation (Side View). The AMS probes (see Figure 4.4-11—Aeroball Probe) use approximately 2500 aeroballs per aeroball stack. The aeroballs are steel balls containing vanadium, which produces a gamma decay signature readily discernable by the measurement software. Each aeroball is approximately 0.067 inch in diameter. The composition of each aeroball is approximately 0.6 percent carbon, 14.5 percent chromium, 1.54 percent vanadium, and 83.36 percent iron.

4.4.6.3   **Excore Neutron Instrumentation**

The signals from the three ranges (source, intermediate, and power) of the neutron flux detectors are used to limit the maximum power output of the reactor within their respective ranges.

The neutron flux instrumentation is installed around the reactor between the vessel and the primary shield and consists of:

- Three source range detectors installed at the major axis of the core.

- Four compensated chambers for the intermediate range installed on the minor axis of the core.

- Four non-compensated bisection chambers for the power range installed on the minor axis of the core.

The three ranges of detectors are used as inputs to monitor neutron flux from a completely shutdown condition to 120 percent of full power, with the capability of recording overpower excursions in excess of 120 percent.

The source range (SR) channels are used for:

- Measurement of the subcritical neutron multiplication during refueling and shutdown operation.

- Acquisition of the neutron flux and increase in neutron flux during the approach to criticality and at zero power.

The intermediate range (IR) channels are used for:

- Acquisition of the neutron flux and increase in neutron flux near criticality, during transition to power, and during power escalation.

- Reactor actuation of reactor trip on low doubling time.

- Actuation of reactor trip on high neutron flux.

- Actuation of RCCA withdrawal block on high neutron flux.

- Input to P5 permissive – "Flux measurement higher than threshold."

- Post accident monitoring.

The output of the power range channels is used for:

- Reactor trip on excore high neutron flux rate of change. The main objective of this function is to cope with a fast reactivity insertion, such as a rod ejection accident.

- Protecting the core against the consequences of adverse power distributions resulting from dropped rods.

- Controlling average coolant temperature.

- Alerting the operator to an excessive azimuthal power imbalance between the quadrants.

- Controlling neutron flux.

- Monitoring reactor power.

Details of the neutron detectors, nuclear instrumentation design, and the control trip logic are given in Chapter 7. The limits on neutron flux operation and trip setpoints are provided in the Technical Specifications.

4.4.6.4   Low DNBR I&C Functions

There are two low DNBR I&C functions:

- Low DNBR protection functions that actuate RT.

- DNBR surveillance functions (LCO).

The use of online DNBR calculations in the protection and surveillance systems allows the DNB design basis to be met by defining a low DNBR RT channel and a low DNBR LCO directly based on the reconstruction of the DNBR in the hot channel.

The low DNBR protection function actuates an RT which protects the fuel against DNB during AOOs, irrespective of the event leading to the uncontrolled decrease in DNBR. The low DNBR surveillance function (LCO) provides sufficient margin to the

DNBR criterion during normal operation in order to accommodate events leading to a significant decrease in DNBR. During normal operation, the DNBR value must be kept above the DNBR LCO threshold so that in case of an AOO for which the low DNBR protection is not effective, the DNB limit is not exceeded (see Reference 9 for additional details).

Exceeding this LCO initiates the following countermeasures:

- At the first threshold, an alarm, blocking of rod cluster control assembly (RCCA) withdrawal, and blocking of load increases.

- At the second threshold, a reactor power reduction by the insertion of rod banks and a matching turbine load reduction.

The I&C algorithms for DNBR protection and surveillance are based on the same principles.

The calculation of the minimum DNBR uses the following parameters:

- Power density distribution in the hot channel. This is directly derived from the neutron instrumentation. The signals of the incore detectors are calibrated in power density units and provide both local power and integrated power over the length of the hot channel.

- Inlet temperature: Derived from the cold leg temperature sensors.

- Pressure: Derived from the primary pressure sensors.

- Core flow rate: Derived from the RCP speed sensors.

The CHF is determined with the applicable CHF correlation using local thermal-hydraulic parameters that are calculated with a simplified, closed-channel model representing the hot channel in the core.

4.4.6.5 High Linear Power Density Functions

There are two high linear power density functions:

- HLPD protection functions that actuate RT.

- LPD surveillance functions (LCO).

The design basis for fuel centerline melting is maintained if the LPD at the hot spot remains lower than the limit.

Thus, the protection and surveillance systems allow the safety criteria concerning fuel melt to be maintained by defining an HLPD RT channel and an LPD LCO channel directly based on the reconstruction of the linear power density at the hot spot.

The HLPD protection function actuates a RT which protects the fuel against centerline melting during accidents, irrespective of the event leading to the uncontrolled increase in linear power density. The LPD surveillance functions LCO to maintain the design basis in case of loss-of-coolant accident (LOCA) (see Reference 9 for additional details).

Violation of this LCO initiates the following countermeasures:

- At the first threshold, an alarm, blocking of RCCA withdrawal or RCCA insertion depending on the axial power shape, and blocking of load increases.

- At the second threshold, a reactor power reduction by the insertion of rod banks and a matching turbine load reduction.

A distortion of the power shape is one possible cause for this limit to be violated. The limit depends on the core axial location (lower for the top core half than for the bottom core half), that is, this surveillance function also limits the axial power shape.

The calculation of the maximum linear power density is based on the readings of the SPND incore instrumentation. The functions are implemented in the PS (refer to Section 7.3.1).

4.4.6.6 Loose Parts Monitoring System

The loose parts monitoring system (LPMS) detects, locates, and analyzes detached or loosened parts and foreign bodies in the reactor coolant system (RCS) and the secondary side of the steam generators during normal plant operation. The LPMS conforms to the guidance provided in Regulatory Guide 1.133 and is described in Section 7.1.

4.4.7 References

1. BAW-10231P-A, Revision 1, "COPERNIC Fuel Rod Design Computer Code," Framatome ANP, January 2004.

2. ANP-10263P-A, Revision 0, "Codes and Methods Applicability Report for the U.S. EPR," AREVA NP Inc., August 2007.

3. BAW-10156-A, Revision 1, "LYNXT Core Transient Thermal-Hydraulic Program," B&W Fuel Company, August 1993.

4. F.W. Dittus, and L.M.K. Boelter, "Heat Transfer in Automobile Radiators of the Tubular Type," California University Publication in Engineering, Volume 2, No. 13, pp. 443-461, 1930.

5. J. Weisman, "Heat Transfer to Water Flowing Parallel to Tube Bundles," Nuclear Science Engineering, Volume 6, pp. 78-79, 1959.

6. W.H. Jens, and P.A. Lottes, "Analysis of Heat Transfer Burnout, Pressure Drop and Density Data for High-Pressure Water," ANL-4627, Argonne National laboratory, Chicago, Illinois, May 1, 1951.

7. ANP-10269P, Revision 0, "The ACH-2 CHF Correlation for the U.S. EPR," AREVA NP Inc., November 2006.

8. BAW-10199P-A, Revision 0, "The BWU Critical Heat Flux Correlations," Framatome Cogema Fuels, August 1996.

9. ANP-10287P, Revision 0, "Incore Trip Setpoint and Transient Methodology for U.S. EPR," AREVA NP Inc., November 2007.

10. BAW-10243P-A, "Statistical Fuel Assembly Hold Down Methodology," Framatome ANP, September 2005.

11. BAW-10147P-A, Revision 1, "Fuel Rod Bowing in Babcock & Wilcox Fuel Designs," Babcock & Wilcox, May 1983.

12. BAW-10186P-A, Revision 2, "Extended Burnup Evaluation," Framatome Cogema Fuels, June 2003.

13. ANP-10282P, Revision 0, "POWERTRAX/E Online Core Monitoring Software for the U.S. EPR," AREVA NP Inc., November 2007.

Table 4.4-1—Thermal and Hydraulic Design Data
Sheet 1 of 2

Parameter	Value
Rated Core Thermal Power	4590 MW$_t$
Number of Loops	4
Nominal System Pressure	2250 psia
Coolant Flow	-
Core Flow Area	63.6 ft^2
Core Average Coolant Velocity	17.7ft/s
Core Average Mass Velocity	2.8 Mlb$_m$/h-ft^2
Vessel Flow Rate (Best Estimate)	184.2.Mlb$_m$/hr
Vessel Thermal Design Flow	478,768 gpm
Vessel Best Estimate Flow	498,964 gpm
Vessel Mechanical Design Flow	538,648 gpm
Coolant Temperature	
Nominal Inlet	563.4°F
Average Rise in Vessel	60.6°F
Average Rise in Core	62.7°F
Average in Core	596.8°F
Average in Vessel	594°F
Heat Transfer	
Heat Transfer Surface Area	86,166 ft^2
Average Core Heat Flux	177,036 Btu/hr-ft^2
Maximum Core Heat Flux (Nominal Operation)	460,294 Btu/hr-ft^2
Fuel Rod Average Linear Power Density	5.08 kW/ft
Fuel Rod Peak Linear Power for Normal Operating Conditions with Uncertainty	13.2 kW/ft
DNB Ratios	
Minimum DNBR Under Nominal Operating Conditions	2.55
DNB Limiting Condition of Operation	2.50

Table 4.4-1—Thermal and Hydraulic Design Data
Sheet 2 of 2

| Parameter	Value
Fuel Assembly	
Number of Fuel Assemblies	241
Fuel Assembly Pitch	8.466 in
Active Fuel Height	165.354 in
Lattice Pitch	0.496 in
Number of Fuel Rods per Assembly	265
Number of Control Rods or Instrumentation Guide Thimbles per Assembly	24
Outside Fuel Rod Diameter	0.374 in
Guide Thimble Diameter	0.490 in

Table 4.4-2—Core Void Fractions

Parameter	Value
Core-Average Void Fraction at the Core Exit	0.000
Average Void Fraction in the Limiting Channel	0.001
Maximum Void Fraction in the Limiting Channel	0.009

Figure 4.4-1—Axial Distribution of Quality and Void Fraction in the Limiting Subchannel
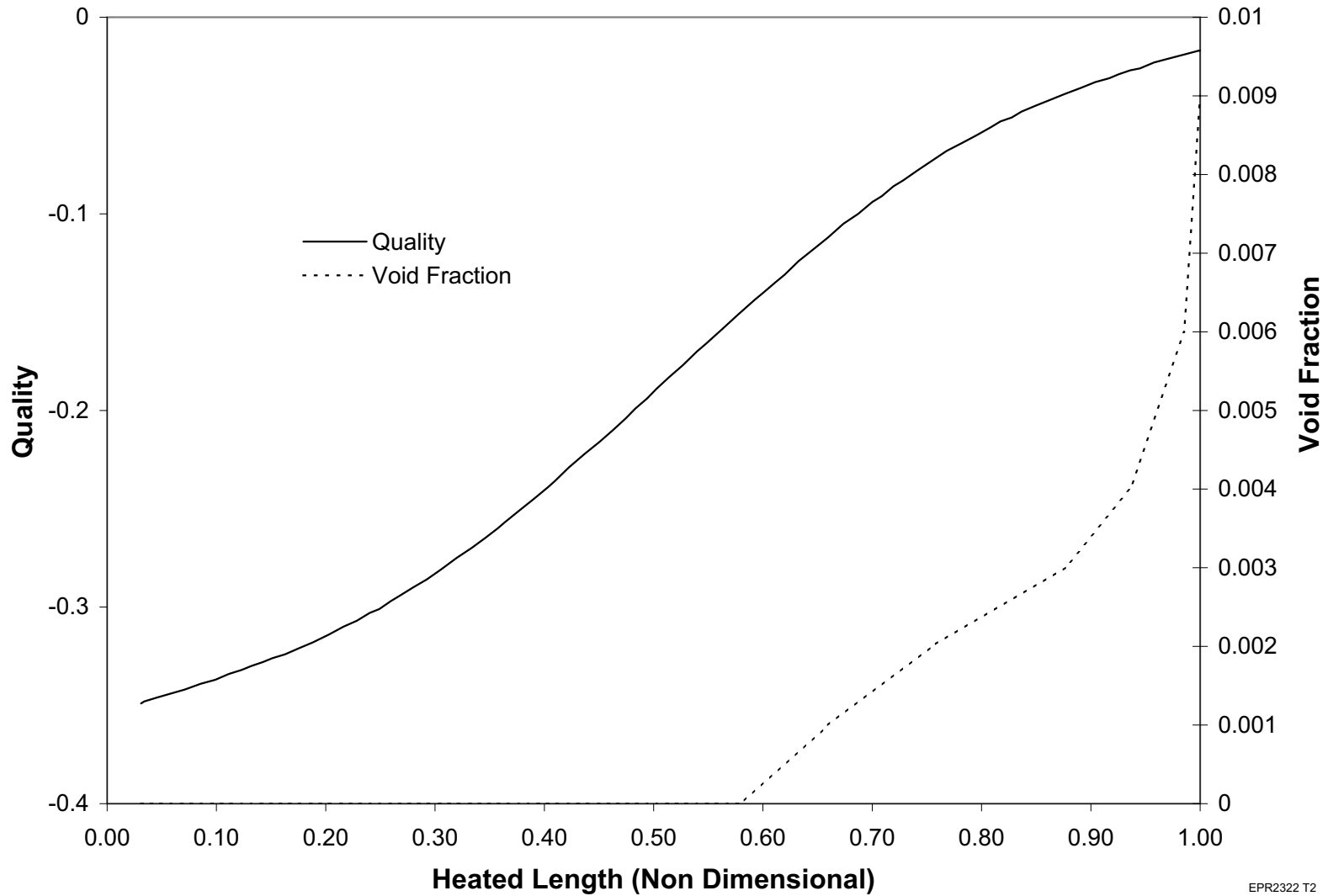
EPR2322 T2

Figure 4.4-2—Radial Distribution of Quality and Void Fraction at the Core Exit
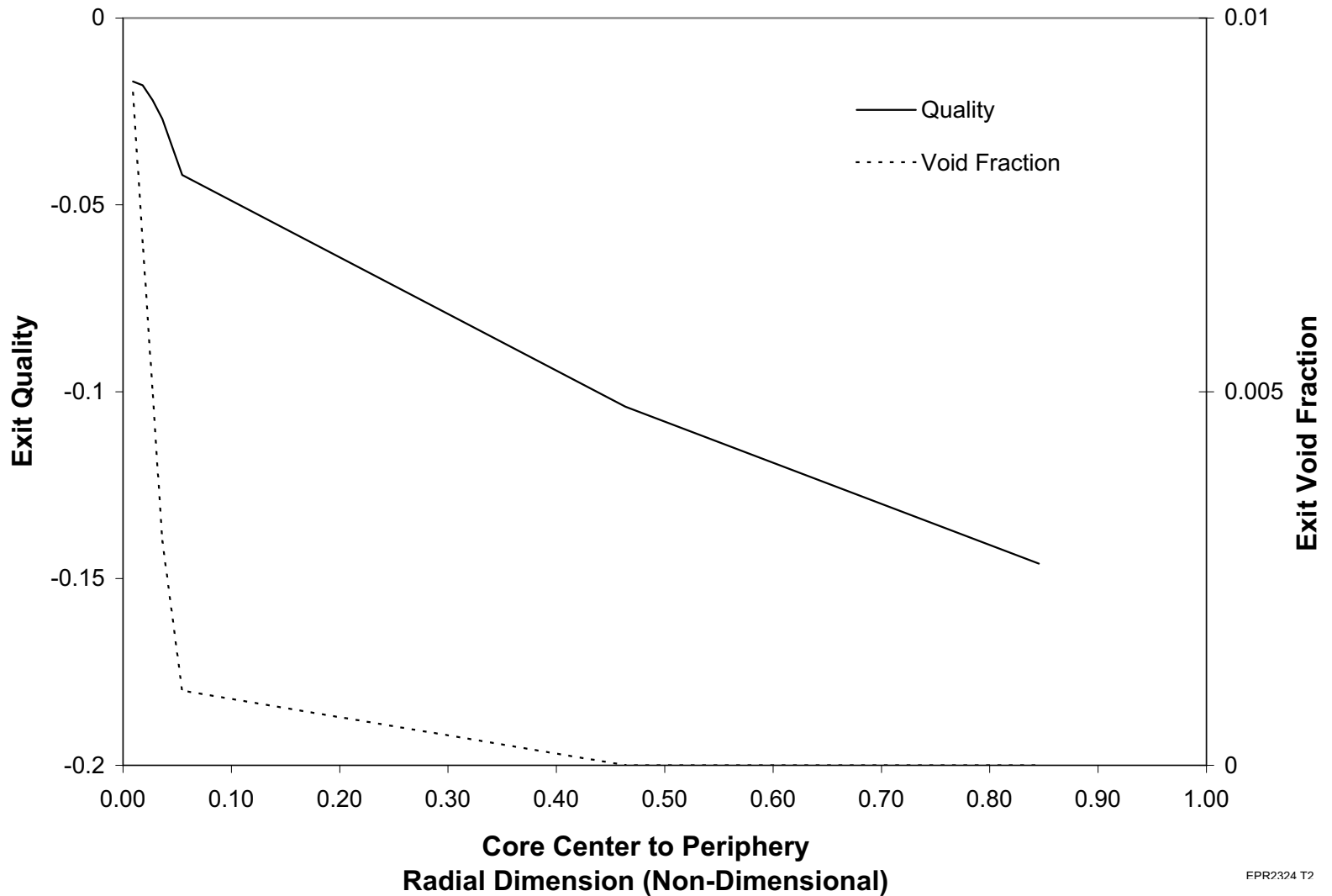
FPR2324 T2

Figure 4.4-3—Assembly Average Flow and Enthalpy Distribution at Core Inlet (1/8 core)

2.9897 563.90	2.9755 563.90	2.9585 563.90	2.9535 563.90	2.9215 563.90	2.8611 563.90	2.7314 563.90	2.7451 563.90	2.7389 563.90
	2.9686 563.90	2.9619 563.90	2.9507 563.90	2.9168 563.90	2.8678 563.90	2.7278 563.90	2.7364 563.90	2.7042 563.90
		2.9563 563.90	2.9249 563.90	2.9043 563.90	2.8158 563.90	2.7545 563.90	2.6346 563.90	2.6379 563.90
			2.9060 563.90	2.8673 563.90	2.7595 563.90	2.7548 563.90	2.7732 563.90	2.5806 563.90
				2.7320 563.90	2.7757 563.90	2.6919 563.90	2.6552 563.90	
					2.7590 563.90	2.5335 563.90	2.5900 563.90	
						2.6964 563.90		

Top = Mass flux (Mlbm/hr/ft^2)
Bottom = Enthalpy (BTU/lbm)

EPR2325 T2

Figure 4.4-4—Assembly Average Flow and Enthalpy Distribution at Core Mid-Plane (1/8 Core)

2.8216 599.59	2.8094 608.48	2.8004 612.64	2.7815 622.94	2.7878 613.68	2.7718 621.01	2.7768 612.73	2.7846 604.05	2.8088 581.14
	2.8065 609.73	2.7884 620.82	2.7932 613.38	2.7739 623.26	2.7830 611.79	2.7756 613.11	2.7747 611.47	2.8082 580.91
		2.7957 612.86	2.7762 623.66	2.7836 613.85	2.7648 623.49	2.7742 612.82	2.7714 612.48	2.8058 581.56
			2.7841 614.32	2.7652 624.37	2.7741 613.84	2.7618 620.52	2.7774 607.13	2.8088 577.26
				2.7734 614.49	2.7569 624.17	2.7750 608.23	2.7986 586.58	
					2.7692 612.84	2.7716 608.86	2.8047 578.92	
						2.8018 581.97		

Top = Mass flux (Mlbm/hr/ft^2)
Bottom = Enthalpy (BTU/lbm)

EPR2330 T2

Figure 4.4-5—Assembly Average Flow and Enthalpy Distribution at Core Exit (1/8 Core)

2.8258 635.21	2.7930 653.15	2.7763 661.52	2.7304 682.71	2.7701 663.46	2.7376 678.22	2.7707 661.25	2.8013 643.94	2.8751 598.15
	2.7880 655.66	2.7412 678.29	2.7724 662.92	2.7277 683.22	2.7760 659.52	2.7695 661.78	2.7730 658.85	2.8756 597.80
		2.7748 661.89	2.7261 684.11	2.7688 663.69	2.7251 683.34	2.7700 661.32	2.7691 660.70	2.8736 599.02
			2.7672 664.66	2.7207 685.34	2.7669 663.33	2.7371 676.94	2.7887 650.26	2.8860 590.47
				2.7647 664.57	2.7199 684.59	2.7859 652.26	2.8593 608.85	
					2.7684 661.39	2.7830 653.27	2.8817 593.66	

Top = Mass flux (Mlbm/hr/ft^2)
Bottom = Enthalpy (BTU/lbm)

2.8729 599.78

EPR2335 T2

Figure 4.4-6—Location of Flow Distribution Device Beneath the Core
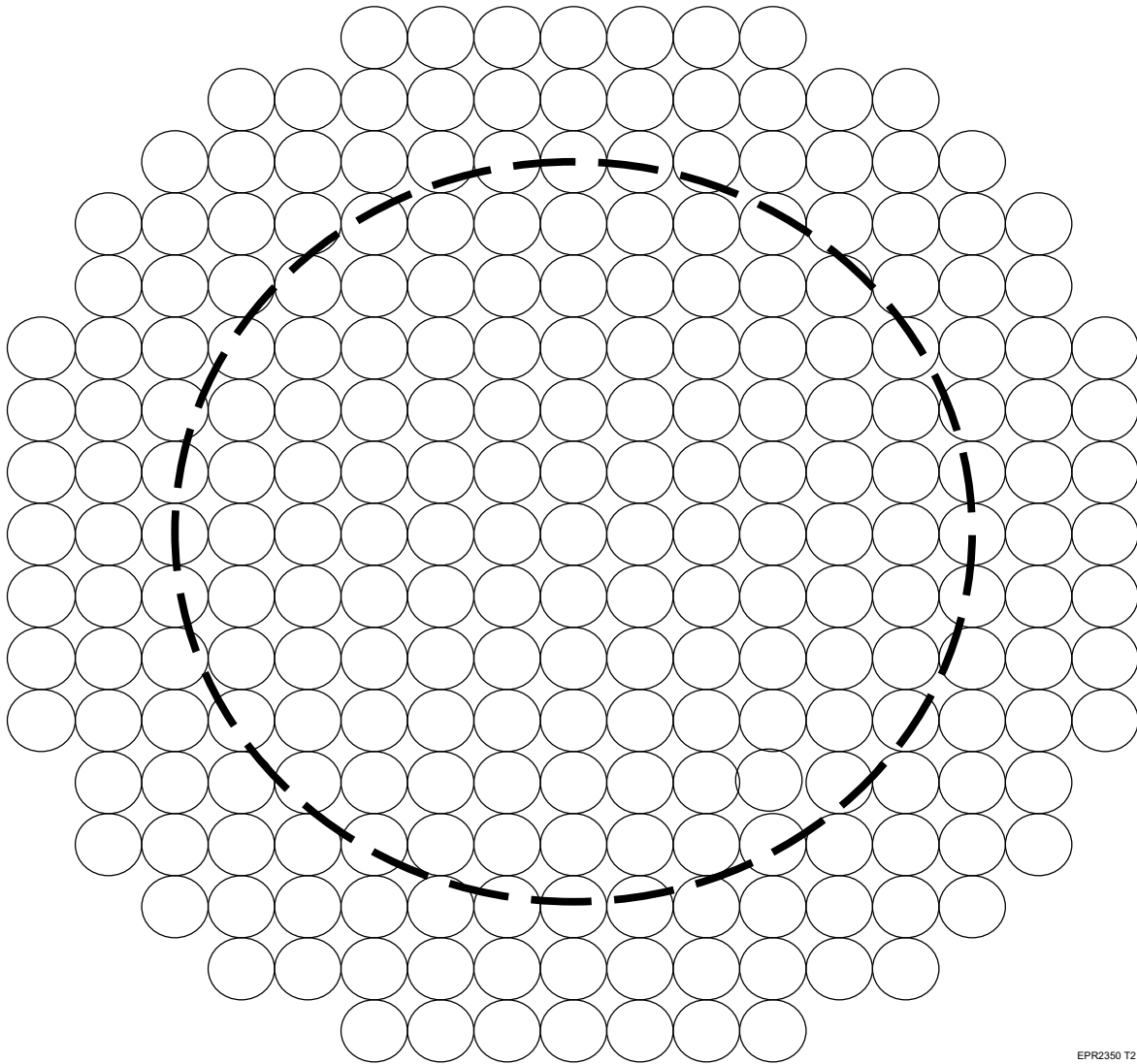

EPR2350 T2

Figure 4.4-7—Average RCS Temperature vs. Core Power
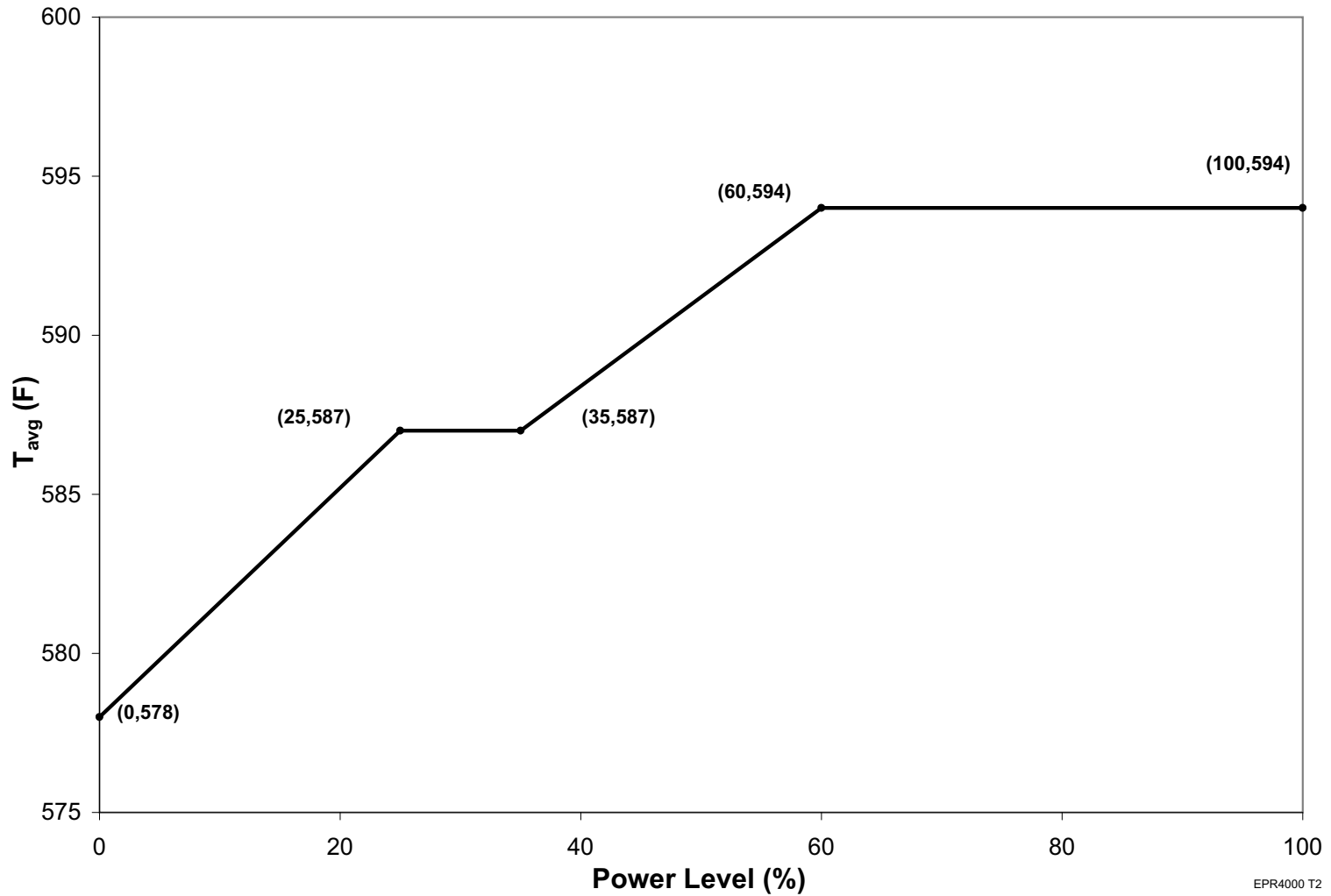
Figure 4.4-8—Arrangement of Incore Instrumentation (Top View)

RCS FLOWS

□ 241 FUEL ASSEMBLIES

○ 40 AEROBALL PROBES
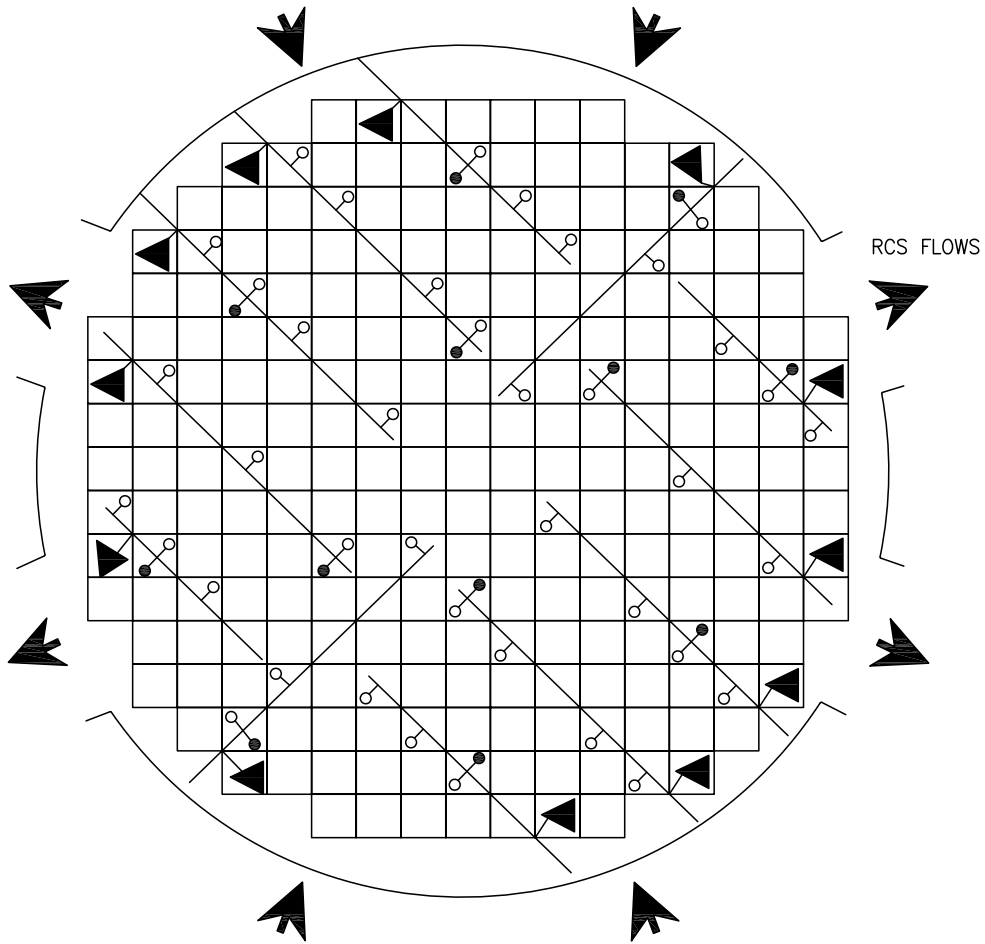
▲ 12 RPV INSTRUMENTATION NOZZLES WITH INSTRUMENTATION LANCES

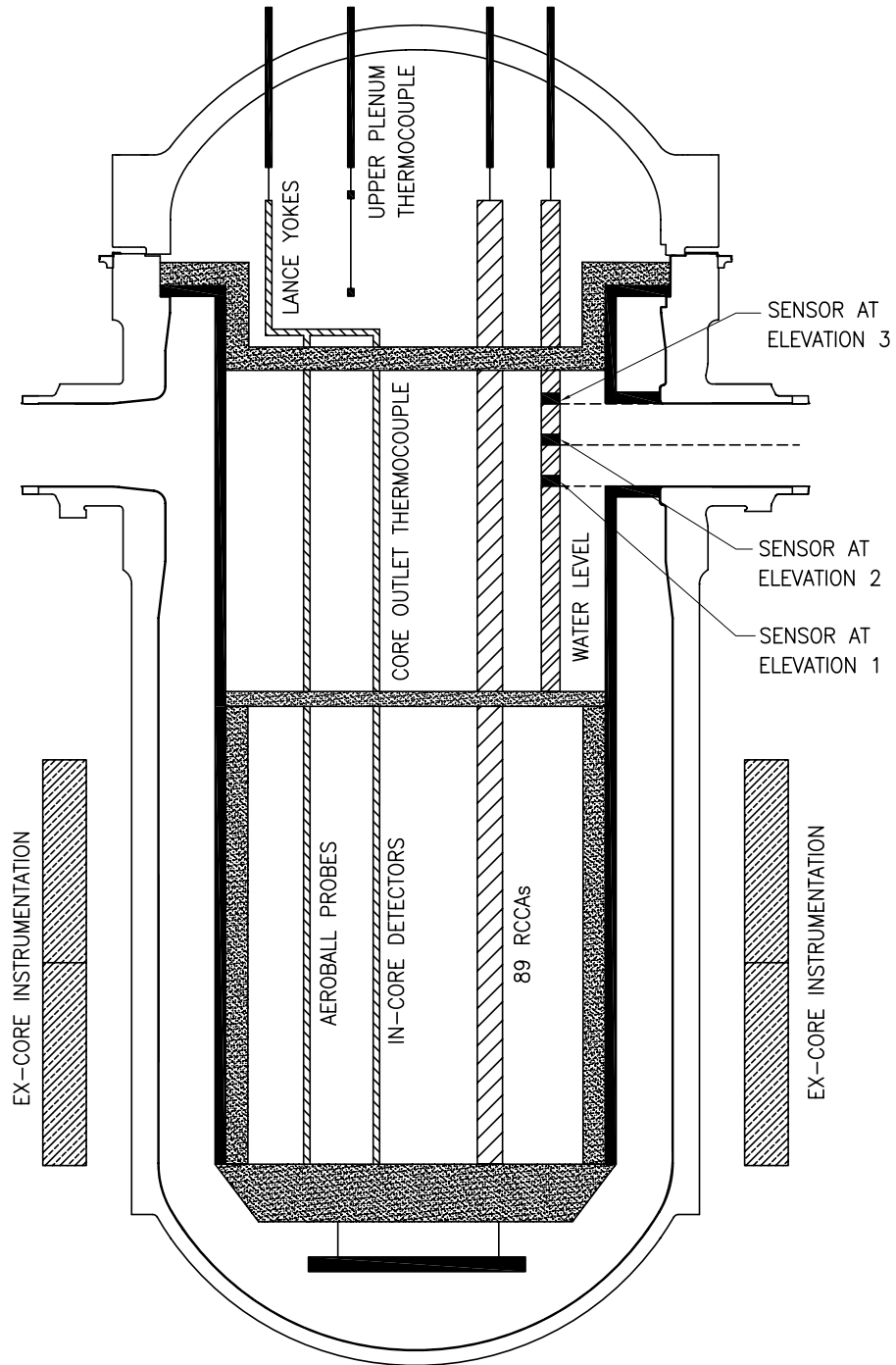● 12 FINGERS WITH POWER DENSITY DETECTORS (PDDs) AND THERMOCOUPLES

╱ 12 LANCE YOKES

EPR2355 T2

Figure 4.4-9—Overview of the Aeroball Measurement System
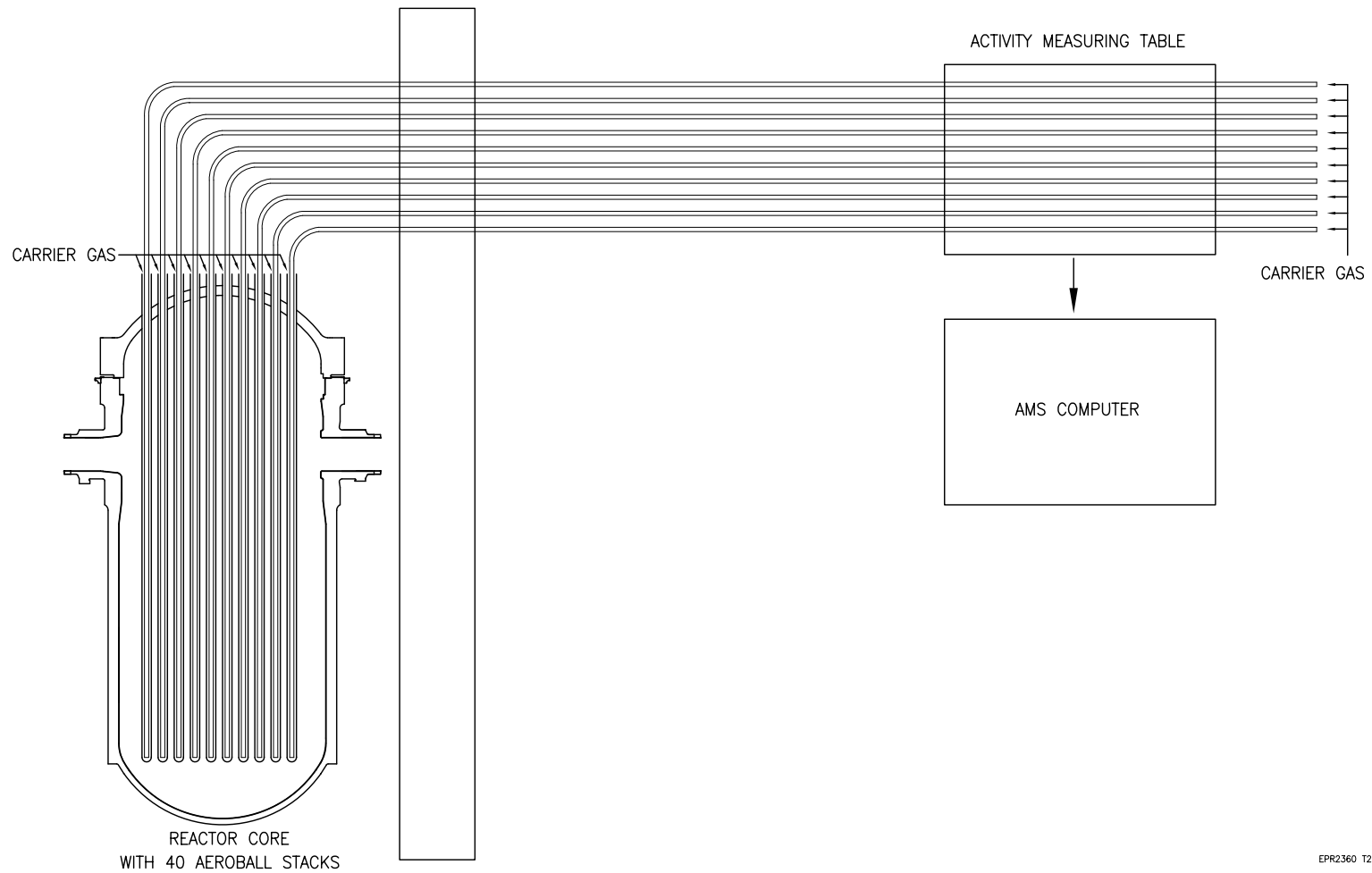
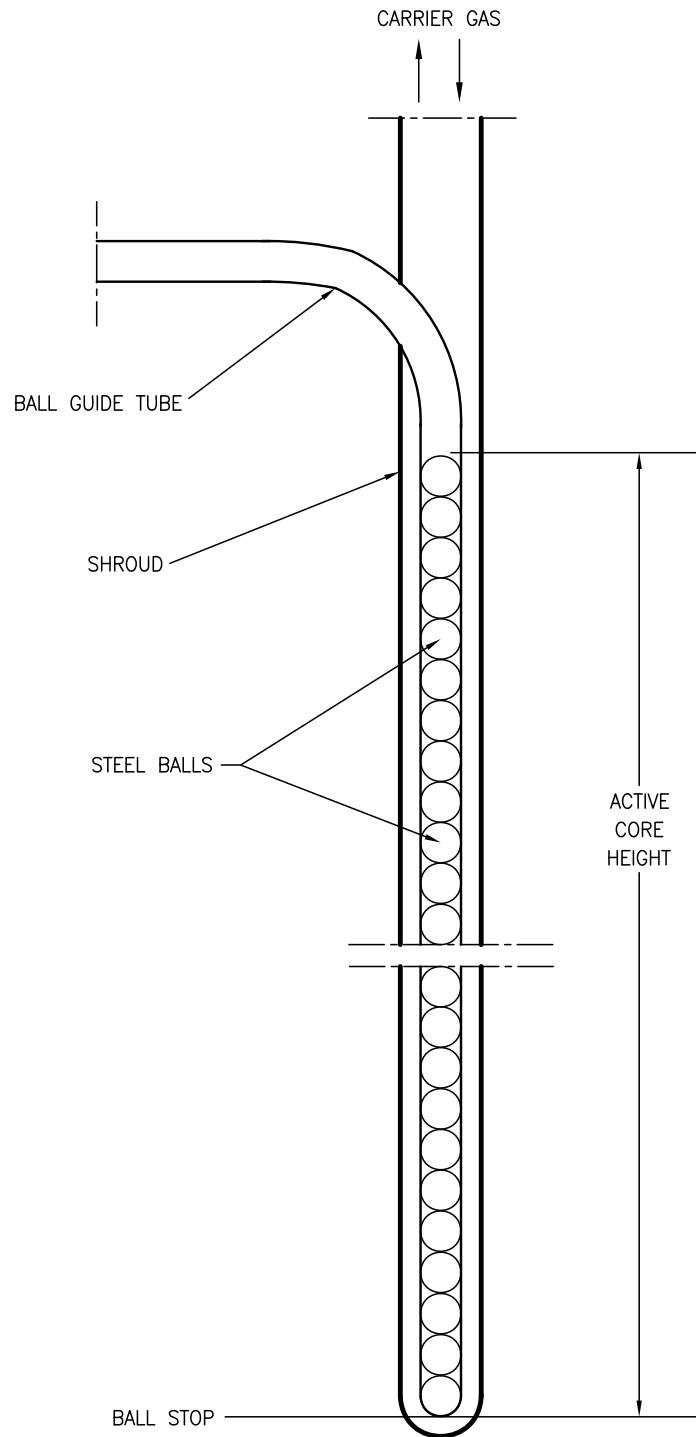**Figure 4.4-10—Arrangement of Incore Instrumentation (Side View)**

EPR2370_T2

Figure 4.4-11—Aeroball Probe

EPR2365 T2